Maximizing the Harvested Energy from Mechanical Random Vibrations with a Matching Network: A Stochastic Analysis

(Article begins on next page)

14 July 2024

Maximizing the harvested energy from mechanical random vibrations with a matching network: a stochastic analysis

Kailing Song
IUSS, University School for Advanced Studies
Pavia, Italy
Politecnico di Torino
Turin, Italy
kailing.song@polito.it

Michele Bonnin and Fabrizio Bonani
Dept. of Electronics and Telecommunications
Politecnico di Torino
Turin, Italy
michele.bonnin@polito.it
fabrizio.bonani@polito.it

Fabio L. Traversa
MemComputing Inc.
San Diego, CA, USA
ftraversa@memcpu.com

Abstract—We consider the problem of modeling and analyzing nonlinear piezoelectric energy harvesters for ambient mechanical vibrations. The equations of motion are derived from the mechanical properties, the characterization of piezoelectric materials, and the circuit description of the electrical load. For random ambient vibrations, modeled as white Gaussian noise, the describing equations become stochastic. The harvester performances are analyzed through time-domain Monte-Carlo simulations. Recently proposed solutions inspired by circuit theory, aimed at improving the power performances of energy harvesters are discussed in presence of random vibrations. Our results show that, even in this case, matching network-based approaches improve significantly the energy harvester performance.

I. INTRODUCTION

Wireless-connected technologies can be nowadays found in every aspect of daily life. The interconnection among the most varied elements, such as computers, printers, handheld communication devices, network appliances and smart systems in general is provided by the internet protocol, while the aforementioned elements form the nodes of the network itself. Among these networked systems, of great practical importance is the interconnection of sensors and actuators, thus forming a Wireless Sensor and Actuators Network (WSAN). WSANs are present whenever there is a need to gather information from the environment, process it, and, consequently, implement actions that appropriately follow from the collected data. These networks may, in general, involve a large (or even huge) number of nodes, connect multi-domain system, and even include both electrical and mechanical systems [1].

Deploying a WSAN requires to tackle a significant number of issues, among which power supply is a major one. In fact, such networked systems are often made of remotely located and/or difficult to access nodes, thus making batteries a possible solution, however impaired by the difficult substitution and by the required physical size, that could be incompatible with the occupation and weight requirements of the node.

On the other hand, in most cases nodes can be effectively designed to require a relatively low power budget as far as the distance among nodes forming the network is not excessive.

Therefore, a self-powering capability implemented scavenging energy from the surrounding environment would be the ideal solution [2]. The term energy harvesting refers to a wide range of technological solutions aimed at realizing small-scale systems with the capability to tap available ambient energy sources, varying from mechanical vibrations to electromagnetic radiation and thermal gradients, and transform the collected energy into usable electric power, fed to the WSAN node either directly or through the use of a buffer battery [3]–[7]. Among the various possible sources, kinetic energy is rather popular as it is widely available and characterized by a significant power density [3]. Several physical principles can be exploited for the conversion of kinetic energy in electrical form, such as electromagnetic transformation and piezoelectric materials. As the latter are in general cheap and allow for the realization of size-effective and reliable transducers, we will focus the attention of piezoelectric harvesters [8]–[11].

One of the main performance limitations for a piezoelectric energy harvester is the sub-optimal energy transfer from the mechanical source to the electrical load, a condition that can be conveniently represented as an impedance mismatch between the electrical equivalent of the entire electro-mechanical system and the load. This suggests to introduce a proper reactive element in parallel with the load, a procedure known in circuit theory as power factor correction [12], [13].

Turning to the vibration source description, in the simplest case of purely sinusoidal vibrations, i.e. when their energy is concentrated at a single frequency, a relatively straightforward analysis of the harvester is possible [12]. However, a more physically sound description takes into account the vibration energy spreading on a relatively wide frequency spectrum, thus requiring the use of a stochastic process to represent the forcing term. For a flat spectrum over a wide enough bandwidth, a white Gaussian noise can be used to conveniently describe the energy source as the theory of stochastic differential equation driven by white Gaussian noise is well developed. However, if the finite, non null noise correlation time cannot be neglected, a colored Gaussian noise process can be used [14], [15].
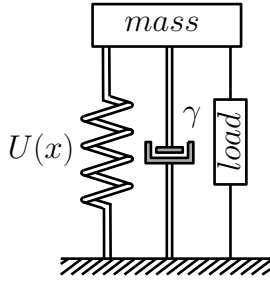
Fig. 1. Schematic representation of an energy harvester for ambient vibrations.

Fig. 2. Representation of a piezoelectric transducer as an electromechanical two-port.

In this contribution, we model a piezoelectric energy harvester subject to random mechanical vibrations, and present novel results through numerical analysis. The mathematical model is derived from the properties of the mechanical part, from the constitutive equations of linear piezoelectric materials, and from the circuit description of the electrical part. The model includes nonlinearities, taking into account nonlinear contributions. Ambient mechanical vibrations are modeled as a white Gaussian noise process. Consequently, the equations of motion are stochastic differential equations, here solved using various numerical integration schemes. Inspired by our recent work on the application of circuit theory to improve the efficiency of energy harvesting systems, we apply a power factor correction solution to the load [12], [16], and we assess the advantage offered by the modified load in terms of output average voltage, output average power and power efficiency. Results show that, even for the case of random mechanical vibrations, the application of power factor correction improves the performances by a significant amount.

II. MODELING NONLINEAR PIEZOELECTRIC ENERGY HARVESTING SYSTEMS

Energy harvesters are multi-domain systems, with mechanical and electrical parts: Fig. 1 provides a schematic energy harvester for ambient mechanical vibrations. The mechanical domain is responsible for capturing the kinetic energy, and is composed of an inertial mass m, connected to a vibrating support through an elastic spring or a cantilever beam. Vibrations of the support produce oscillations of the mass, here converted into electrical power exploiting a piezoelectric transducer. We remark that other transduction mechanisms lead to very similar equations, thus a similar analysis can be performed [12].

The equation of motion for the oscillating system is readily derived from classical mechanics

$$m\ddot{x} + \gamma\dot{x} + U'(x) + F_{tr}(t) = F_{vib}(t) \tag{1}$$

where m is the inertial mass, x is the displacement with respect to the equilibrium position, dots denote derivative with respect to time, γ is the damping coefficient, $U(x) = k_1 x^2/2 + k_3 x^4/4$ is the elastic potential of the spring (or the cantilever), and the $'$ denotes derivation with respect to the argument. For $k_3 = 0$ the harvester is linear, otherwise it is nonlinear. Finally, $F_{tr}(t)$ is the force exerted on the mechanical system by the transducer, and $F_{vib}(t)$ is the external force modeling ambient vibrations.
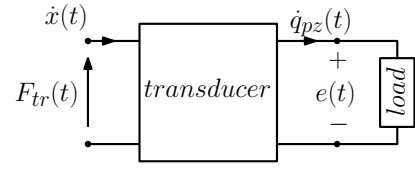
In a piezoelectric transducer, a layer of piezoelectric material is deposited on the oscillating structure (the spring or the cantilever beam). Stress and strain induced in the layer by mechanical deformation, are converted into electrical power. Starting from the characterization of piezoelectric materials the following relationships between mechanical and electrical quantities are derived [12], [16]–[18]

$$F_{tr} = \alpha\,e \tag{2a}$$
$$q_{pz} = \alpha\,x - C_{pz}\,e \tag{2b}$$

where α is the electro-mechanical coupling (in N/V or As/m), C_{pz} is the electrical capacitance of the piezoelectric layer, and q_{pz} and e are the charge and voltage, respectively. The transducer can be represented as an electro-mechanical two-port, with mechanical quantities at the input, and electrical quantities at the output, see Fig. 2 and [18]. The output voltage e is used to supply power to an electrical load.

Substituting (2a) into (1), rewriting as a system of first order differential equations and differentiating (2b) with respect to time we obtain:

$$\dot{x} = y \tag{3a}$$
$$\dot{y} = -\frac{1}{m}\,U'(x) - \frac{\gamma}{m}y - \frac{\alpha}{m}\,e + \frac{1}{m}\,F_{vib}(t) \tag{3b}$$
$$\dot{e} = \frac{\alpha}{C_{pz}}\,y - \frac{1}{C_{pz}}\dot{q}_{pz} \tag{3c}$$

In circuit theory, a load, normally modeled as a resistor, is any electrical component absorbing power from the preceding circuit (Fig. 3(a)). Previous studies [12], [16] showed that a fundamental factor limiting the harvested power and power efficiency, is the impedance mismatch between the mechanical and the electrical domains of the harvester. Impedance mismatch, a classical problem in electrical and electronic engineering, can be taken care of exploiting a solution inspired by RF electronics: to interpose a matching network between the source (the electromagnetic harvester) and the resistive load so that the power delivered to the load is maximized. Different types of matching network exist. Here we consider a simple matching network composed by two reactive elements, an inductor L_S and a capacitor C_P connected as in Fig. 3(b). This solution is called low-pass L-matching network, because of the arrangement of the reactive elements, and because at very low frequency the inductor behaves as a short circuit.

To assess whether the application of the matching network improves the power performances of the energy harvester, we should calculate the average power $P_{out} = G v_{rms}^2$ absorbed
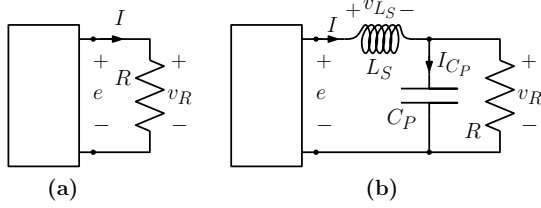
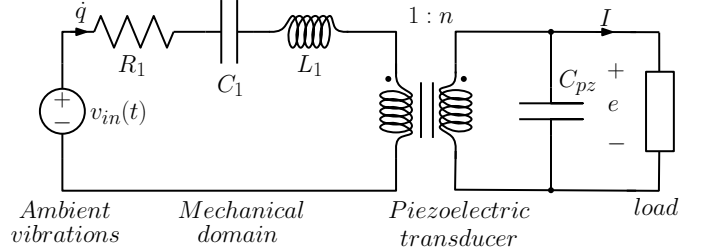Fig. 3. Electrical load connected to the electromagnetic energy harvester. (a) Resistive load. (b) Resistive load with low-pass L-matching network.

Fig. 4. Equivalent circuit for a piezoelectric nonlinear energy harvester with a resistive-inductive load.

by the load, where v_{rms} is the root mean square value of the load voltage:

$$v_{R\,rms} = \sqrt{\langle v_R^2(t) \rangle} \tag{4}$$

and $\langle \cdot \rangle$ denotes the mean value (expectation) operator. For the resistive load of Fig. 2(a), $v_R = e$, application of Ohm law yields $\dot{q}_{pz} = G v_R$, where $G = R^{-1}$ is the load conductance. Substituting into (3) results in the state equations

$$\dot{x} = y \tag{5a}$$

$$\dot{y} = -\frac{1}{m} U'(x) - \frac{\gamma}{m} y - \frac{\alpha}{m} v_R + \frac{1}{m} F_{vib}(t) \tag{5b}$$

$$\dot{v}_R = \frac{\alpha}{C_{pz}} y - \frac{G}{C_{pz}} v_R \tag{5c}$$

Conversely, for the matched load shown in Fig. 3(b), $\dot{q}_{pz} = I$. Using the constitutive relationship of the linear inductor $v_{L_S} = L_S \dot{I}$ and applying Kirchhoff voltage law gives $L_S \dot{I} + v_R - e = 0$. Similarly, using the constitutive relationship for a linear capacitor $I_{C_P} = C_P \dot{v}_R$ and using Kirchhoff current law yields $-I + C_P \dot{v}_R + G v_R = 0$. Combining these equations together with (1) and the time derivative of (2b) yields

$$\dot{x} = y \tag{6a}$$

$$\dot{y} = -\frac{1}{m} U'(x) - \frac{\gamma}{m} y - \frac{\alpha}{m} \alpha e + \frac{1}{m} F_{vib}(t) \tag{6b}$$

$$\dot{e} = \frac{\alpha}{C_{pz}} y - \frac{1}{C_{pz}} I \tag{6c}$$

$$\dot{I} = \frac{1}{L_S} (e - v_R) \tag{6d}$$

$$\dot{v}_R = \frac{1}{C_P} (I - G v_R) \tag{6e}$$

III. EQUIVALENT CIRCUIT MODELING

State equations (5) and (6) can be used to derive an equivalent circuit model, i.e. an electrical circuit retaining the behavior of the original electro-mechanical systems as it is described by the same equations. The equivalent circuit shown in Fig. 4, is obtained exploiting mechanical to electrical analogies [16]: the variable substitutions are summarized in Table I. Ambient mechanical vibrations are modeled as an independent, ideal voltage source. The oscillating structure is equivalent to an electrical oscillator, where inductor L_1 plays the role of the inertial mass, and capacitor C_1 has a nonlinear voltage-charge characteristic, representing the nonlinear elastic potential. Internal friction is described by resistor R_1. Finally, an ideal transformer with turns ratio $1 : n$ ($n = \alpha^{-1}$) in parallel with a linear capacitor C_{pz} is used to model the piezoelectric transducer.

IV. STOCHASTIC DIFFERENTIAL EQUATIONS

Ambient mechanical vibrations are described as stochastic processes. In particular, if the energy is distributed over a relatively large frequency interval, vibrations can be modeled as uncorrelated white Gaussian noise, and the differential equations (5) or (6) become stochastic differential equations (SDEs).

Let $(\Omega, \mathcal{F}, P)$ be a probability space, where Ω is the sample space, $\mathcal{F} = (\mathcal{F}_t)_{t \geq 0}$ is a filtration, i.e. the σ-algebra of all the events, and P is a probability measure. Let $W_t = W(t)$ be a one dimensional Wiener process, characterized by $\langle W_t \rangle = 0$, covariance $\text{cov}(W_t, W_s) = \langle W_t W_s \rangle = \min(t, s)$ and $W_t \sim \mathcal{N}(0, t)$, where symbol $\sim$ means "distributed as", and $\mathcal{N}(0, t)$ denotes a normal distribution with zero expectation.

A d-dimensional system of SDEs driven by the one-dimensional Wiener process W_t takes the form

$$d\boldsymbol{X}_t = \boldsymbol{a}(\boldsymbol{X}_t) dt + \boldsymbol{B}(\boldsymbol{X}_t) dW_t \tag{7}$$

where $\boldsymbol{X}_t : \Omega \mapsto \mathbb{R}^d$ is a vector valued stochastic process, i.e. a vector of random variables parameterized by $t \in T$. The parameter space T is usually the half-line $[0, +\infty[$. The vector valued function $\boldsymbol{a} : \mathbb{R}^d \mapsto \mathbb{R}^d$ is called the drift, while function $\boldsymbol{B} : \mathbb{R}^d \mapsto \mathbb{R}^d$ is the diffusion. If $\boldsymbol{B}(\boldsymbol{X}_t)$ is constant, then noise is un-modulated or additive, otherwise it is modulated or multiplicative. Functions $\boldsymbol{a}(\boldsymbol{X}_t)$ and $\boldsymbol{B}(\boldsymbol{X}_t)$ are measurable functions, satisfying a global Lipschitz and a linear growth conditions, to ensure the existence and uniqueness solution theorem [19].

Equations (5)-(6) are conveniently rewritten as SDEs for a-dimensional variables (including a-dimensional time). The d-dimensional system of SDEs can be recast in the form:

$$d\boldsymbol{X}_t = (\boldsymbol{A}\,\boldsymbol{X}_t + \boldsymbol{n}(\boldsymbol{X}_t))\,dt + \boldsymbol{B}\,dW_t \tag{8}$$

where the constant matrix $\boldsymbol{A} \in \mathbb{R}^{d,d}$ and function $\boldsymbol{n} : \mathbb{R}^d \mapsto \mathbb{R}^d$ are, respectively, the linear and nonlinear terms of the drift, and the diffusion matrix $\boldsymbol{B}$ is constant (un-modulated noise).

We introduce linear transformed variables $\boldsymbol{y} = \boldsymbol{P}\boldsymbol{x}$, where $\boldsymbol{P} \in \mathbb{R}^{d,d}$ is a constant matrix. In order for the transformation to be invertible, $\boldsymbol{P}$ must be regular. Using Itô rule [19], [20], the following SDEs for the stochastic processes $\boldsymbol{y}$ are obtained:

$$d\boldsymbol{Y}_t = \left(\boldsymbol{P}\boldsymbol{A}\boldsymbol{P}^{-1}\boldsymbol{Y}_t + \boldsymbol{P}\boldsymbol{n}(\boldsymbol{P}^{-1}\boldsymbol{Y}_t)\right)dt + \boldsymbol{P}\boldsymbol{B}\,dW_t \quad (9)$$

Time variable change in SDEs is not trivial. Consider the time change $t' = \tau(t) = \omega\,t$, with $\omega > 0$. If $\boldsymbol{Y}_t$ solves (9), then $\boldsymbol{Y}_\tau$ solves

$$d\boldsymbol{Y}_\tau = \left(\boldsymbol{P}\boldsymbol{A}\boldsymbol{P}^{-1}\boldsymbol{Y}_\tau + \boldsymbol{P}\boldsymbol{n}(\boldsymbol{P}^{-1}\boldsymbol{Y}_\tau)\right)d\tau + \boldsymbol{P}\boldsymbol{B}\,dW_\tau \quad (10)$$

Using the change of time theorem for Itô integrals (see [19], page 156) the time scaled Wiener process is

$$W_{\tau(t)} \sim \sqrt{\tau'(t)}\,W_t = \sqrt{\omega}\,W_t \quad (11)$$

where, again, symbol $\sim$ means "distributed as". Using $d\tau = \omega\,dt$, and defining $\widetilde{\boldsymbol{Y}}_t = \boldsymbol{Y}_\tau$ we have that $\widetilde{\boldsymbol{Y}}_t$ is a weak solution for the SDE

$$d\widetilde{\boldsymbol{Y}}_t = \omega\left(\boldsymbol{P}\boldsymbol{A}\boldsymbol{P}^{-1}\widetilde{\boldsymbol{Y}}_t + \boldsymbol{P}\boldsymbol{n}(\boldsymbol{P}^{-1}\widetilde{\boldsymbol{Y}}_t)\right)dt + \sqrt{\omega}\boldsymbol{P}\boldsymbol{B}\,dW_t \quad (12)$$

Being a weak solution implies that $\widetilde{\boldsymbol{Y}}$ and $\boldsymbol{Y}$ have the same probability distribution. In most applications this information is the most important, because the interest is not on the detailed solution for a specific realization of the Wiener process, but rather on expected quantities that can be calculated using the probability density function.

To derive the a-dimensional SDEs for the energy harvester with the resistive and the matched load, we assume a nonlinear elastic potential of the form $U(x) = k_1 x^2/2 + k_3 x^4/4$ and we model ambient vibrations as white Gaussian noise with variance D^2. Consequently, the equivalent circuit in Fig. 4 includes a voltage source $v_{in}(t) = D dW_t$ and a nonlinear capacitor with nonlinear voltage-charge characteristic $v_C(q) = q^2/(2C_1) + q^4/(4C_3)$.

For the circuit with resistive load, system (5) is rewritten as the SDEs (8), with $\boldsymbol{X}_t = [q, i, v_R]^T$, $\boldsymbol{n}(\boldsymbol{X}_t) = [0, -q^3/C_3, 0]^T$, $\boldsymbol{B} = [0, D, 0]^T$ and

$$\boldsymbol{A} = \begin{bmatrix} 0 & 1 & 0 \\ -\frac{1}{L_1 C_1} & -\frac{R_1}{L_1} & -\frac{\alpha}{L_1} \\ 0 & \frac{\alpha}{C_{pz}} & -\frac{G}{C_{pz}} \end{bmatrix} \quad (13)$$

The SDEs for a-dimensional variables are obtained introducing the diagonal matrix $\boldsymbol{P} = \text{diag}[Q^{-1}, TQ^{-1}, C_{pz}Q^{-1}]$, where Q is a normalization factor that has dimension of a charge, and T is the time scaling factor $T = 1/\omega = \sqrt{L_1 C_1}$. Similarly, for the equivalent circuit with the matched load we

Parameter	Value
R_1	6.9366 Ω
C_1	5.874 μF
L_1	1 H
C_{pz}	80.08 nF
R	1 MΩ
n	37.4254

TABLE II
VALUES OF CIRCUIT COMPONENTS, BASED ON [22]

have $\boldsymbol{X}_t = [q, i, e, I, v_R]^T$, $\boldsymbol{n}(\boldsymbol{X}_t) = [0, -q^3/C_3, 0, 0, 0]^T$, $\boldsymbol{B} = [0, D, 0, 0, 0]^T$ and

$$\boldsymbol{A} = \begin{bmatrix} 0 & 1 & 0 & 0 & 0 \\ -\frac{1}{L_1 C_1} & -\frac{R_1}{L_1} & -\frac{\alpha}{L_1} & 0 & 0 \\ 0 & \frac{\alpha}{C_{pz}} & 0 & -\frac{1}{C_{pz}} & 0 \\ 0 & 0 & \frac{1}{L_S} & 0 & -\frac{1}{L_S} \\ 0 & 0 & 0 & \frac{1}{C_P} & -\frac{G}{C_P} \end{bmatrix} \quad (14)$$

SDEs for a-dimensional variables are obtained using the diagonal matrix $\boldsymbol{P} = \text{diag}[Q^{-1}, TQ^{-1}, C_{pz}Q^{-1}, TQ^{-1}, C_{pz}Q^{-1}]$.

V. RESULTS

To verify whether the matched load increases the harvested power and power efficiency, we have performed Monte Carlo simulations for the energy harvester with both the resistive and the matched load. The SDEs have been solved numerically using different numerical integration schemes, including Euler-Maruyama[1], strong order 1 stochastic Runge-Kutta, and weak order 2 stochastic Runge-Kutta [21]. Time simulation length was $\Delta t = 10^4$ s, with a constant time integration step $\delta t \approx 30$ μs. The relatively small time step implies the absence of any significant difference in the solutions obtained using different numerical integration methods. For our numerical simulations, we used the circuit component values reported in [22], and here summarized in Table II. For the nonlinear voltage-charge characteristic of the capacitor, it was assumed $C_3 = Q^2 \cdot C_1$, where $Q = 1$ C. Expected quantities where obtained averaging over one hundred simulations.

Fig. 5 shows the root mean square (rms) value for the output voltage $v_{R\,rms} = \sqrt{\langle v_R^2(t)\rangle}$, versus the value of the load resistance R, for the resistive load case.

For comparison, the output voltage rms value for the harvester with matched load, versus the values of the matching network parameters L_S and C_P, is shown in Fig. 6. Optimal values of the parameters maximizing the harvested voltage are clearly seen. As well as the advantage of the matched load, which offers a much higher output voltage than the simple resistive load. It is worth mentioning that the very high optimum value for the matching inductance: $L_S^{opt} = 303.7273$ H, is a consequence of the normalization used, that fixes $L_1 = 1$ H.

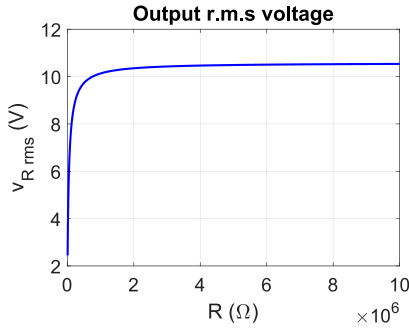[1]Since noise is un-modulated, Euler-Maruyama and Milstein numerical schemes coincide.

Fig. 5. Root mean square value for the output voltage v_R, versus the resistance of the load for the resistive load setup. Parameter $D = 50$mV, other parameters value are those of table II.

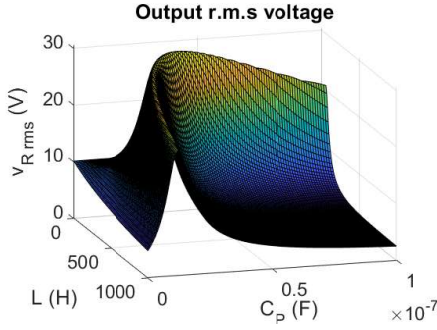Fig. 6. Root mean square value for the output voltage v_R, versus the matching network parameters L_S and C_P. Parameter $D = 50$mV, other parameters value are those of table II.

Fig. 7 shows a comparison of the average harvested power by the harvester with resistive and matched load, versus the noise intensity. Optimum values of parameters of the matching network, determined from fig. 6 are: $L_S^{opt} = 303.7$ H, and $C_P^{opt} = 23.31$ pF. The matched solution offers about nine times more power with respect to the simple resistive load.

To calculate the power efficiency of the harvester, we need the average power injected by the noise. This is easily calculated using stochastic calculus. Here we give the details for the matched load case, the same procedure can be applied
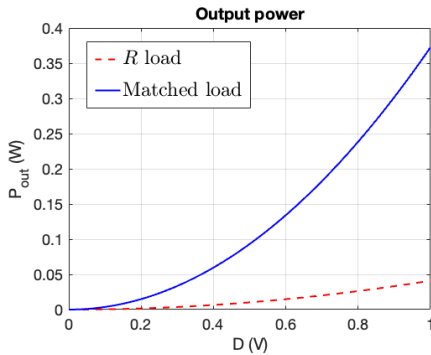

Fig. 7. Comparison of the average harvested power for the harvester with resistive load and with matched load, versus the noise intensity. Parameters of the matching network are $L_S^{opt} = 303.7$H, $C_P^{opt} = 23.31$pF. Parameter $D = 50$ mV.

Load	$v_{R\,rms}$	P_{out}	ε
Resistive load	10.1315 V	0.10265 mW	8.21%
Matched load	30.5210 V	0.93153 mW	74.52 %

TABLE III
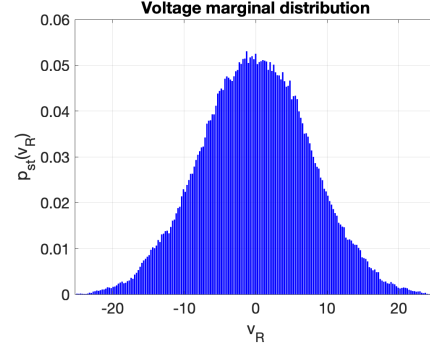PERFORMANCES COMPARISON FOR A SIMPLE RESISTIVE LOAD, AND A MATCHED LOAD.

Fig. 8. Stationary marginal probability density function for the output voltage $p_{st}(v_R)$, for the energy harvester with resistive load. Parameter $D = 50$ mV.

for the resistive load yielding similar results. For the equivalent circuit with matched load, the total energy stored in the circuit is the sum of the energies stored in the reactive elements L_1, C_1, L_S and C_P. Notice that the ideal transformer does not store energy, it only transfers electrical power from the primary to the secondary windings. The total energy is

$$E_{tot}(t) = \frac{1}{2}L_1 i(t)^2 + U(q(t)) + \frac{1}{2}L_S I(t)^2 + \frac{1}{2}C_P v_R(t)^2 \tag{15}$$

Differentiating using Itô rule, using (6) and taking expectation we obtain

$$\left\langle \frac{dE}{dt} \right\rangle = -R_1 \langle i^2 \rangle - G \langle v_R^2 \rangle + \frac{D^2}{2L_1} \tag{16}$$

where we used the property of Itô integral: $\langle i(t)\, dW_t \rangle = 0$.

Equation (16) implies that the circuit reaches a steady state, where the power dissipated by the resistors R_1 and R, is balanced by the power injected by noise $P_{in} = D^2/(2L_1)$. Power efficiency is the ratio between the power transferred to the load and the power injected by noise, that is:

$$\varepsilon = \frac{2L_1 G \langle v_R^2 \rangle}{D^2} \tag{17}$$

Table III shows the rms output voltage, average harvested power and power efficiency for the harvester with resistive and matched load. Application of a simple matching network improves the harvester performances by a significant amount. In particular, both the average harvested power and power efficiency for the system with matched load are nine times higher than those for the resistive load.

Finally, we discuss the role of nonlinearity. Fig. 8 and 9 show the marginal probability density function for the output voltage $p_{st}(v_R)$, for the energy harvester with resistive and with matched load, respectively. The stationary marginal distribution is calculated from the numerical simulations as
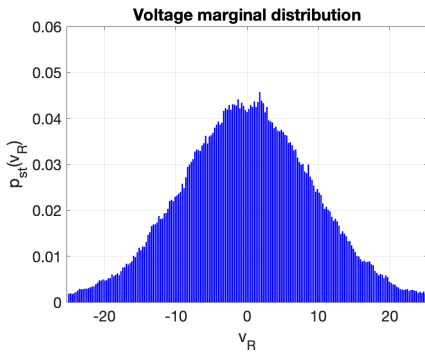
Fig. 9. Stationary marginal probability density function for the output voltage $p_{st}(v_R)$, for the energy harvester with matched load. Parameter $D = 50$ mV.

follows. We perform a long simulation and we eliminate the transient period, retaining only the long time behavior. The probability to find the system in state $v_R + dv_R$ is calculated as the fraction of samples in that interval, normalized to the total number of samples that have been retained. Both figures show a clear resemblance with a Gaussian distribution, suggesting that the nonlinearity plays a marginal role. In fact, the SDEs obtained linearizing the harvester equations around the origin (the only stable equilibrium point of the underlying deterministic system) describe an Ornstein-Uhlenbeck process, and it is well known that the stationary distribution of the Ornstein-Uhlenbeck process is a normal centered at the origin. Therefore we conclude that, at least for reasonable values of the noise intensity, the excitation is not strong enough to induce significant nonlinear effect in the harvester. To observe such nonlinear effects, either very strong excitations should be considered, or a different, softer spring should be used.

VI. Conclusions

Piezoelectric energy harvesters are micro-scale electro-mechanical systems designed to transform ambient mechanical vibrations into electrical energy. As such, they are well suited to provide a power energy source to electronic circuits, sensors and actuators wirelessly connected to form a WSAN.

In terms of the harvested energy effectiveness, the impedance mismatch between the mechanical and the electrical parts of the harvester is the main limiting factor. A possible workaround is to exploit power factor correction methods from circuit theory to minimize this effect. In qualitative terms, interposing a reactive element between the equivalent electrical source and the load amounts to reduce the lag between the voltage across and the current through the load, thereby increasing the absorbed power.

In this work we analyzed a nonlinear piezoelectric energy harvester for ambient mechanical vibrations exploiting stochastic methods to account for their non uniform spectral power distribution. The equations of motion have been derived from the mechanical properties, the characteristic equations of linear piezoelectric materials and the electrical circuit description of the load. In the case of random ambient vibrations described as white Gaussian noise, the resulting stochastic differential equations have been solved numerically,

and expected quantities have been calculated using Monte-Carlo simulation techniques.

Our analysis shows that the power factor corrected solution offers better performances in terms of output voltage, output average absorbed power and power efficiency. The output voltage is increased by almost three times, while absorbed power and power efficiency by almost nine times.

References

[1] R. Verdone, D. Dardari, G. Mazzini, and A. Conti, *Wireless Sensor and Actuator Networks*. Academic Press, 2008.

[2] M. T. Penella-López and M. Gasulla-Forner, *Powering Autonomous Sensors An Integral Approach with Focus on Solar and RF Energy Harvesting*. Springer London, Limited, 2011.

[3] S. Roundy, P. K. Wright, and J. M. Rabaey, *Energy scavenging for wireless sensor networks*. Springer, 2003.

[4] J. A. Paradiso and T. Starner, "Energy scavenging for mobile and wireless electronics," *IEEE Pervasive computing*, vol. 4, no. 1, pp. 18–27, 2005.

[5] S. P. Beeby, M. J. Tudor, and N. White, "Energy harvesting vibration sources for microsystems applications," *Measurement science and technology*, vol. 17, no. 12, p. R175, 2006.

[6] P. Mitcheson, E. Yeatman, G. Rao, A. Holmes, and T. Green, "Energy harvesting from human and machine motion for wireless electronic devices," *Proceedings of the IEEE*, vol. 96, no. 9, pp. 1457–1486, sep 2008.

[7] X. Lu, P. Wang, D. Niyato, D. I. Kim, and Z. Han, "Wireless networks with RF energy harvesting: A contemporary survey," *IEEE Communications Surveys & Tutorials*, vol. 17, no. 2, pp. 757–789, 2015.

[8] A. Khaligh, P. Zeng, and C. Zheng, "Kinetic energy harvesting using piezoelectric and electromagnetic technologies—state of the art," *IEEE transactions on industrial electronics*, vol. 57, no. 3, pp. 850–860, 2009.

[9] H. Vocca, I. Neri, F. Travasso, and L. Gammaitoni, "Kinetic energy harvesting with bistable oscillators," *Applied Energy*, vol. 97, pp. 771–776, 2012.

[10] X. Wen, W. Yang, Q. Jing, and Z. L. Wang, "Harvesting broadband kinetic impact energy from mechanical triggering/vibration and water waves," *ACS nano*, vol. 8, no. 7, pp. 7405–7412, 2014.

[11] Y. Fu, H. Ouyang, and R. B. Davis, "Nonlinear dynamics and triboelectric energy harvesting from a three-degree-of-freedom vibro-impact oscillator," *Nonlinear Dynamics*, vol. 92, no. 4, pp. 1985–2004, 2018.

[12] M. Bonnin, F. L. Traversa, and F. Bonani, "Leveraging circuit theory and nonlinear dynamics for the efficiency improvement of energy harvesting," *Nonlinear Dynamics*, vol. 104, no. 1, pp. 367–382, 2021.

[13] D. Huang, S. Zhou, and G. Litak, "Analytical analysis of the vibrational tristable energy harvester with a RL resonant circuit," *Nonlinear Dynamics*, vol. 97, no. 1, pp. 663–677, 2019.

[14] M. F. Daqaq, "Response of uni-modal Duffing-type harvesters to random forced excitations," *Journal of sound and Vibration*, vol. 329, no. 18, pp. 3621–3631, 2010.

[15] M. Bonnin, F. L. Traversa, and F. Bonani, "Analysis of influence of nonlinearities and noise correlation time in a single-DOF energy-harvesting system via power balance description," *Nonlinear Dynamics*, vol. 100, no. 1, pp. 119–133, mar 2020.

[16] ——, "An impedance matching solution to increase the harvested power and efficiency of nonlinear piezoelectric energy harvesters," *Energies*, vol. 15, no. 8, p. 2764, 2022.

[17] S. Priya and D. J. Inman, *Energy harvesting technologies*. Springer, 2009, vol. 21.

[18] M. Bonnin and K. Song, "Frequency domain analysis of a piezoelectric energy harvester with impedance matching network," *Energy Harvesting and Systems*, vol. at press, 2022.

[19] B. Øksendal, *Stochastic Differential Equations*, 6th ed. Berlin: Springer–Verlag, 2003.

[20] C. W. Gardiner *et al.*, *Handbook of stochastic methods*. Springer Berlin, 1985, vol. 3.

[21] S. Särkkä and A. Solin, *Applied stochastic differential equations*. Cambridge University Press, 2019, vol. 10.

[22] Y. Yang and L. Tang, "Equivalent circuit modeling of piezoelectric energy harvesters," *Journal of intelligent material systems and structures*, vol. 20, no. 18, pp. 2223–2235, 2009.